Spring 2015

Simulation of electronic and optical properties of graphene

Biao Leng
New Jersey Institute of Technology

Copyright Warning & Restrictions

The copyright law of the United States (Title 17, United States Code) governs the making of photocopies or other reproductions of copyrighted material.

Under certain conditions specified in the law, libraries and archives are authorized to furnish a photocopy or other reproduction. One of these specified conditions is that the photocopy or reproduction is not to be "used for any purpose other than private study, scholarship, or research." If a, user makes a request for, or later uses, a photocopy or reproduction for purposes in excess of "fair use" that user may be liable for copyright infringement,

This institution reserves the right to refuse to accept a copying order if, in its judgment, fulfillment of the order would involve violation of copyright law.

Please Note: The author retains the copyright while the New Jersey Institute of Technology reserves the right to distribute this thesis or dissertation

Printing note: If you do not wish to print this page, then select "Pages from: first page # to: last page #" on the print dialog screen

ABSTRACT

SIMULATION OF ELECTRONIC AND OPTICAL PROPERTIES OF GRAPHENE

by
Biao Leng

Graphene is a recently discovered two-dimensional crystal. Due to its excellent electronic properties, transport properties, optical properties, and many other features, it has tremendous potential for applications in many areas. This thesis discusses the structure and properties of graphene using several different models of graphene and carries out detailed theoretical studies and calculations of its electronic and optical properties. Using two modules of Materials Studio, CASTAP and Doml^3, four graphene models have been constructed. Their electronic and optical properties have also been calculated via these two modules. By comparing the results of calculations with experimental results and the literature, the influence of different structures of these models has been discussed.

SIMULATION OF ELECTRONIC AND OPTICAL PROPERTIES OF GRAPHENE

by
Biao Leng

A Thesis
Submitted to the Faculty of
New Jersey Institute of Technology
in Partial Fulfillment of the Requirements for the Degree of
Master of Science in Materials Science and Engineering

Interdisciplinary Program in Materials Science and Engineering

May 2015

APPROVAL PAGE

SIMULATION OF ELECTRONIC AND OPTICAL PROPERTIES OF GRAPHENE

Biao Leng

Dr. N. M. Ravindra, Thesis Advisor — Date
Director of Materials Science and Engineering Program, NJIT

Dr. Michael Jaffe, Committee Member — Date
Research Professor, Department of Biomedical Engineering, NJIT

Mr. Peter Kaufman, Committee Member — Date
President and Chief Technical Officer, Public Service Solutions Inc.

Dr. Halina Opyrchal, Committee Member — Date
Senior University Lecturer, Department of Physics, NJIT

BIOGRAPHICAL SKETCH

Author: Biao Leng

Degree: Master of Science

Date: May 2015

Undergraduate and Graduate Education:

- Master of Science in Materials Science and Engineering,
  New Jersey Institute of Technology, Newark, NJ, 2015

- Bachelor of Science in Applied Physics,
  Sichuan University, Chengdu, People's Republic of China, 2013

Major: Materials Science and Engineering

This thesis is dedicated to my parents; it was their support that gave me the ability to complete this work.

ACKNOWLEDGMENTS

I would like to thank my professor and advisor Dr. N.M. Ravindra for his great kindness and support throughout my thesis. I would also like to thank my committee members: Dr. Halina Opyrchal, Dr. Michael Jaffe and Mr. Peter Kaufman for their insights and suggestions.

I thank my parents for their love and their support.

TABLE OF CONTENTS

TABLE OF CONTENTS
（Continued）

LIST OF FIGURES

LIST OF FIGURES
（Continued）

CHAPTER 1

INTRODUCTION

1.1 Objective

Since the discovery of graphene, it has been intensely researched in recent decades due to its unique structure and properties. Enormous amounts of theoretical and experimental work has been done. However, in order to study its properties, we have to synthesize graphene first, and it is expensive. Even after more than 10 years of developing different synthesis methods, the cost of making 1g of graphene can still be as expensive as $150 or more. In order to not to waste this expensive material, a necessary and low-cost method to study the target material is needed, which is simulation and modeling. By simulating the target material utilizing appropriate software, we can build its model first and study its properties before we synthesize it so that we can test the structure and reduce costs in processing and subsequently manufacturing. We can also compare the outcomes of simulations and the results of experiments to see the similarities and differences between theoretical and experimental work. Materials Studio 7.0 has been used as simulation software in this work to study the electronic and optical properties of graphene with different structures.

1.2 Structure of Graphene

Graphene has a two-dimensional crystalline structure. It is an allotrope of carbon. Carbon atoms are densely packed in a regular sp2-bonded atomic-scale hexagonal pattern in graphene. Graphene can be described as a one-atom thick layer of graphite. [1]. It is the basic structural element of other allotropes, including graphite, fullerenes and carbon nanotubes. Perfect pure graphene is strong, light, nearly transparent and an excellent conductor of heat and electricity. Graphene has significant stability due to its tightly packed carbon atoms and a sp2 orbital hybridization – a combination of orbitals s, p_x and p_y that constitute the σ-bond. The final p_z electron makes up the π-bond. The excellent electrical properties of graphene are due to the half-filled band that permits free-moving electrons. Each atom has four bonds, one σ bond with each of its three neighbors and one π-bond that is oriented out of plane. The atoms are about 1.42 Å apart [1].

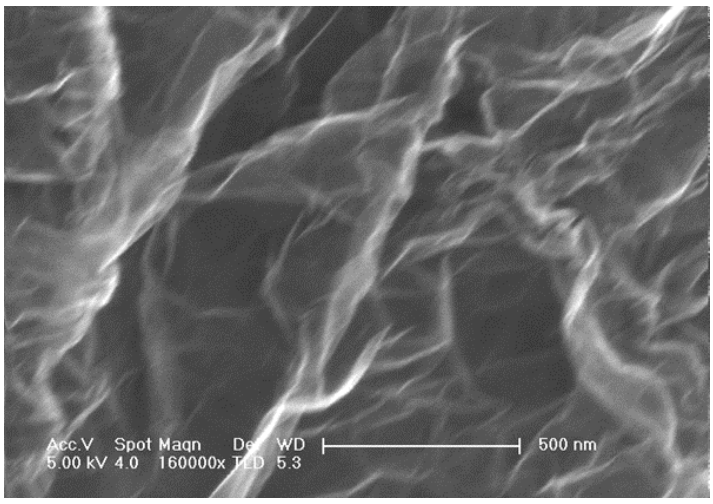

Figure 1.1 SEM micrograph of monolayer graphene.

Source: Factory, A.M.-G. Single Layer Graphene (Graphene Factory). 2015 [cited 2015 April]; Available from: http://www.acsmaterial.com/product.asp?cid=25&id=137 [2].

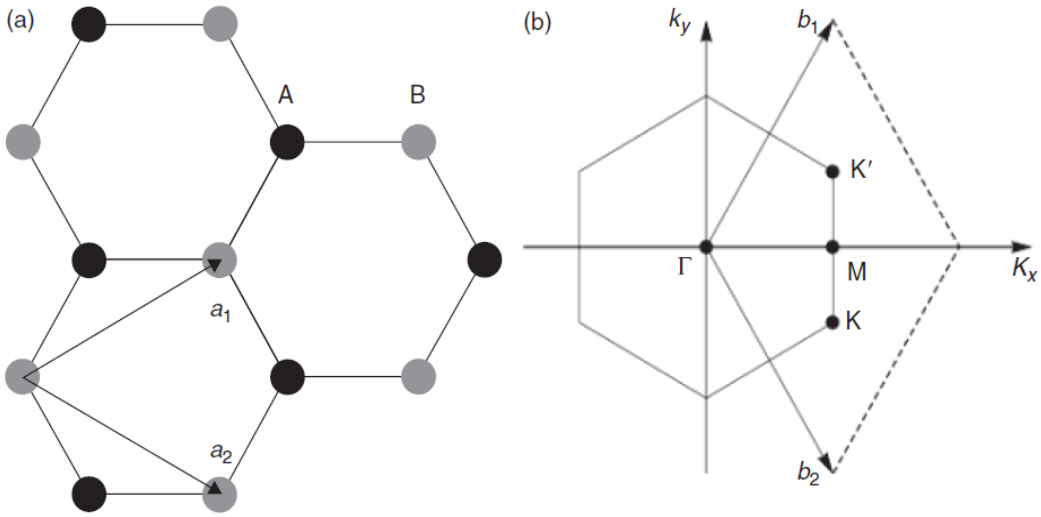

Figure 1.2 A honeycomb lattice of graphene, sub-lattices A and B are shown as black and grey. (b) Reciprocal lattice vectors and some special points in the Brillouin zone.

Source: Katsnelson, M. I., & Katsnel′son, M. I. (2012). Graphene: carbon in two dimensions. Cambridge University Press [3].

Graphene has a honeycomb crystal lattice as shown in Figure 1.2 (a); it has two atoms in each elementary cell which belong to two sublattices A and B.

$$\overrightarrow{a1} = \frac{a}{2}(3, \sqrt{3}), \qquad \overrightarrow{a2} = \frac{a}{2}(3, -\sqrt{3}) \tag{1.1}$$

where, $a \approx 1.42\text{Å}$ is the nearest distance between carbon atoms in the honeycomb lattice. It corresponds to a conjugated carbon-carbon bond.

As for the reciprocal lattice in Brillouin zone,

$$\overrightarrow{b1} = \frac{2\pi}{3a}(1, \sqrt{3}), \qquad \overrightarrow{b2} = \frac{2\pi}{3a}(1, -\sqrt{3}) \tag{1.2}$$

where, $a \approx 1.42\text{Å}$ is the nearest distance between carbon atoms in the honeycomb lattice.

1.3 Electronic Properties of Graphene

The band gap for perfect graphene is zero, because its conduction and valence bands meet at the Dirac points at the Fermi level. The Dirac points are six locations in momentum space, on the edge of the Brillouin zone; they can be divided into two non-equivalent sets of three points- K and K'.

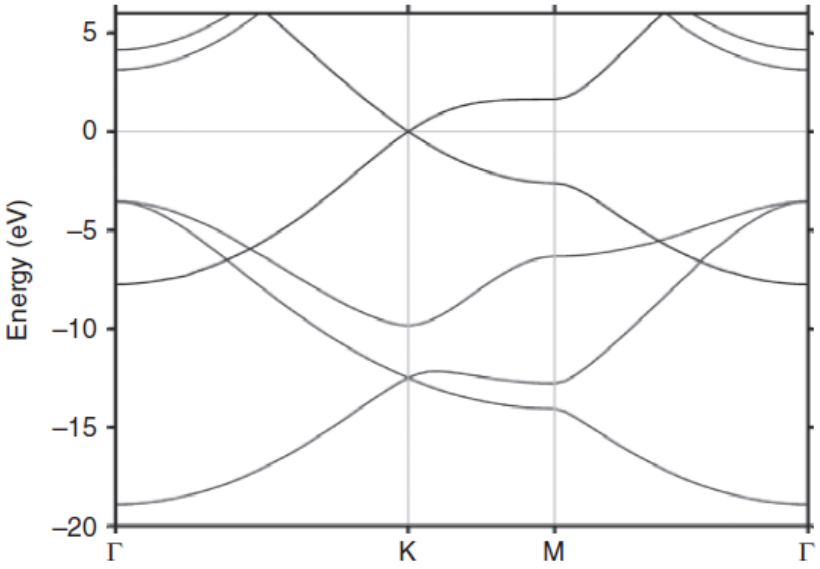

Figure 1.3 Band structure of graphene.

Source: Katsnelson, M. I., & Katsnel′son, M. I. (2012). Graphene: Carbon in two dimensions. Cambridge University Press [3].

In momentum space, the positon of K and K' are given by:

$$\mathrm{K} = (\frac{2\pi}{3a}, \frac{2\pi}{3\sqrt{3}a}), \qquad \mathrm{K}' = (\frac{2\pi}{3a}, -\frac{2\pi}{3\sqrt{3}a}) \tag{1.3}$$

In real space, the 3 nearest vectors are:

$$\delta_1 = \frac{a}{2}(1, \sqrt{3}), \qquad \delta_2 = \frac{a}{2}(1, -\sqrt{3}), \qquad \delta_3 = -a(1,0) \tag{1.4}$$

where, $a \approx 1.42\text{Å}$ is the nearest distance between carbon atoms in the honeycomb lattice.

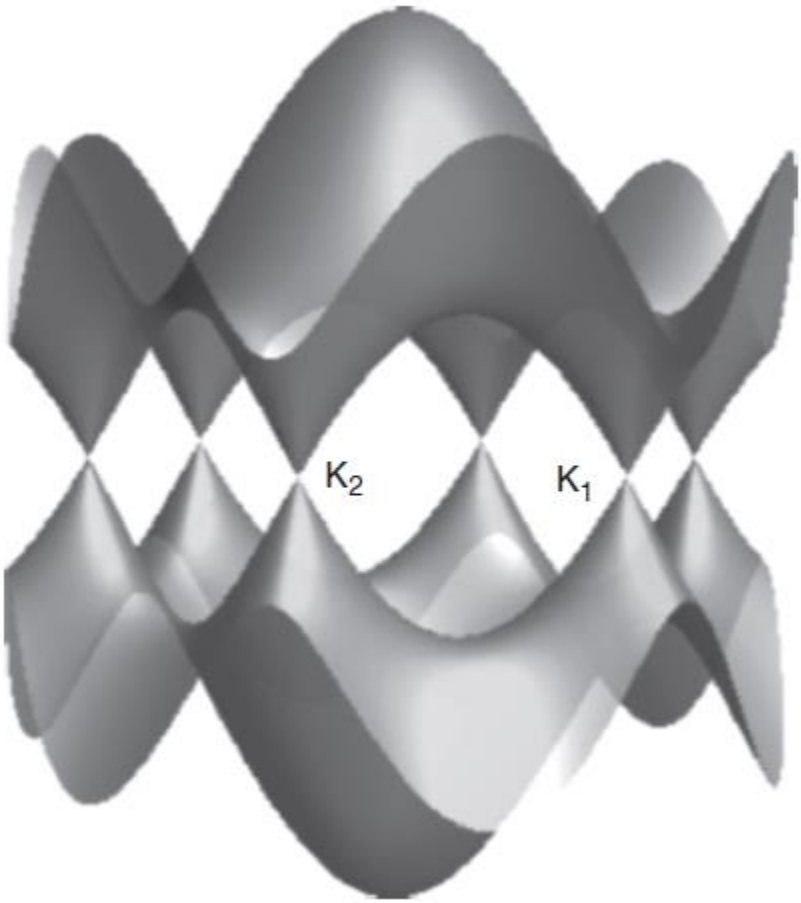

Figure 1.4 Electron energy spectrum of graphene in the nearest-neighbor approximation.

Source: Katsnelson, M. I., & Katsnel′son, M. I. (2012). Graphene: carbon in two dimensions. Cambridge University Press [3].

At the near-neighbor of K and K', the electrons' linear dispersion relation is

$$E = \hbar v_F \sqrt{k_x^2 + k_y^2} \tag{1.5}$$

where the wavevector k is measured from the Dirac points[4].

Electron transfer measurement results show that, at room temperature, graphene has surprisingly high electron mobility. Its value exceeds

$15{,}000\text{cm}^2\,\text{V}^{-1}\text{S}^{-1}$. Symmetry from the measured conductivity data obtained show that the mobility of holes and electrons should be equal. Between 10 K and 100 K [5], the mobility is almost independent of temperature, and may be subject to scattering defects within a graphene lattice. At room temperature and carrier density of $10^{12}/\text{cm}^2$, the scattering in graphene is due to phonon scattering. The mobility of charge carriers in graphene is $200{,}000\text{cm}^2\,\text{V}^{-1}\text{S}^{-1}$. This value corresponds to a resistivity of 10^{-6} Ω • cm, slightly less than the resistivity of silver ~ 1.59×10^{-6} Ω • cm. At room temperature, the lowest resistivity material is silver [6]. Therefore, graphene is an excellent conductor. For graphene sheet on SiO_2, the scattering of phonons in graphene is relatively larger than in SiO_2, the upper limit of which leads to a mobility of $40{,}000\text{cm}^2\,\text{V}^{-1}\text{S}^{-1}$ [7]. Due to the chemical dopant in graphene, the carrier mobility might be affected; so the experiment can detect the degree of influence. Experimentalists, with the option of using a variety of gas molecules (some donor; some acceptor) incorporated in graphene, have found that even when the chemical dopant concentration exceeds $10^{12}/\text{cm}^2$, the carrier mobility changes slightly. Due to the two-dimensional nature of graphene, scientists believe that the charge fraction of the apparent charge (apparent charge in a low-dimensional material is less than the quasi-particle quantum units) will occur in graphene. Therefore, graphene may be a suitable material for any desired quantum computer subcomponents [8].

1.4 Optical Properties of Graphene

Graphene sheet has a unique ability to absorb a rather large 2.3% of white light, especially considering that it is only 1 atom thick. This is due to its aforementioned electronic properties; the electrons act like massless charge carriers with very high mobility. Not long ago, it has been proved that the amount of white light absorbed is based on the Fine Structure Constant, rather than being dictated by material specifics. Adding another layer of graphene increases the amount of white light absorbed by approximately the same value (2.3%). Graphene's opacity of $\pi\alpha \approx 2.3\%$ equates to a universal dynamic conductivity value of $G = 2e^2/4\hbar$ (±2-3%) over the visible frequency range.

Due to these impressive characteristics, it has been observed that once optical intensity reaches a certain threshold (known as the saturation fluence), saturable absorption takes place (very high intensity light causes a reduction in absorption) [9].

CHAPTER 2

THEORY AND BACKGROUND

2.1 Density functional theory

Density functional theory (DFT) is a computational quantum mechanical modeling method used in physics, chemistry and materials science to investigate molecules and electronic structure of many-body systems. Originally, density functional theory of quantum systems was proposed in 1927 by Thomas and Fermi. It was not accurate enough at that time. However, their approach illustrates the way how density functional theory works. Although density functional theory has its conceptual roots in the Thomas–Fermi model, DFT was not considered as a firm theory until the two Hohenberg–Kohn theorems (H–K) [10].

Hohenberg–Kohn Theorems

1. If there are two systems of electrons, one trapped in a potential $v_1(\vec{r})$ and the other in $v_2(\vec{r})$, with both of them having the same ground-state density $n(\vec{r})$, then necessarily,

$$v_1(\vec{r}) - v_2(\vec{r}) = const. \qquad (2.1)$$

In other words, the potential and all the properties of the system are mainly determined by the ground state density uniquely including the many-body wave function.

In particular, the "HK" functional, defined as $F[n] = T[n] + U[n]$ is a universal functional of the density (not depending explicitly on the external potential) [11].

2. For any positive integer N and potential $v(\vec{r})$, a density functional $F[n]$ exists such that,

$$E_{(v,N)}[n] = F[n] + \int v(\vec{r})n(\vec{r})d^3r \qquad (2.2)$$

obtains its minimal value at the ground-state density of N electrons in the potential $v(\vec{r})$. The minimal value of $E_{(v,N)}[n]$ is then the ground state energy of this system [11].

The first H–K theorem demonstrates that the ground state properties of a many-electron system are uniquely determined by an electron density that depends on only three spatial coordinates. It lays the groundwork for reducing the many-body problem of N electrons with 3N spatial coordinates to three spatial coordinates, through the use of functionals of the electron density. This theorem can be extended to the time-dependent domain to develop time-dependent density functional theory (TDDFT), which can be used to describe excited states [10].

The second H–K theorem defines an energy functional for the system and proves that the correct ground state electron density minimizes this energy functional.

Within the framework of Kohn–Sham DFT (KS DFT), the intractable many-body problem of interacting electrons in a static external potential is reduced to a tractable problem of non-interacting electrons moving in an effective potential. The effective potential includes the external potential and the

effects of the Coulomb interactions between the electrons, e.g., the exchange and correlation interactions. Modeling the latter two interactions becomes the difficulty within the KS DFT. The simplest approximation is the local-density approximation (LDA), which is based on exact exchange energy for a uniform electron gas, which can be obtained from the Thomas–Fermi model, and from fits to the correlation energy for a uniform electron gas. Non-interacting systems are relatively easy to solve as the wave function can be represented as a Slater determinant of orbitals. Further, the kinetic energy functional of such a system is known exactly. The exchange-correlation part of the total-energy functional remains unknown and must be approximated.

Another approach, less popular than the KS DFT but arguably more closely related to the spirit of the original H-K theorems, is the orbital-free density functional theory (OFDFT), in which approximate functionals are also used for the kinetic energy of the non-interacting system [12].

2.2 Kohn–Sham Equations

In physics and quantum chemistry, specifically density functional theory, the Kohn–Sham equation is the Schrödinger equation of a fictitious system (the "Kohn–Sham system") of non-interacting particles (typically electrons) that generate the same density as any given system of interacting particles. The Kohn–Sham equation is defined by a local effective (fictitious) external potential in which the non-interacting particles move, typically denoted as $v_s(r)$ or $v_{eff}(r)$, called the Kohn–Sham potential. As the particles in the Kohn–Sham system are non-interacting Fermions, the Kohn–Sham wave function is a single Slater determinant constructed from a set of orbitals that are the lowest energy solutions to:

$$\left(-\frac{\hbar^2}{2m}\nabla^2 + v_{\text{eff}}(\mathbf{r})\right)\phi_i(\mathbf{r}) = \varepsilon_i\phi_i(\mathbf{r}) \tag{2.3}$$

This eigenvalue equation is the typical representation of the Kohn–Sham equations. Here, ε_i is the orbital energy of the corresponding Kohn–Sham orbital, φ_i, and the density for an N-particle system is:

$$\rho(\mathbf{r}) = \sum_{i}^{N} |\phi_i(\mathbf{r})|^2. \tag{2.4}$$

The Kohn–Sham equations are named after Walter Kohn and Lu Jeu Sham, who introduced the concept at the University of California, San Diego in 1965 [13, 14].

2.3 Local-Density Approximations (LDA)

Local-density approximations (LDA) are a class of approximations to the exchange–correlation (XC) energy functional in density functional theory (DFT) that depend solely on the value of the electronic density at each point in space (and not, for example, derivatives of the density or the Kohn–Sham orbitals). Many approaches can yield local approximations to the XC energy. However, overwhelmingly successful local approximations are those that have been derived from the homogeneous electron gas (HEG) model. In this regard, LDA is generally synonymous with functionals based on the HEG approximation, which are then applied to realistic systems (molecules and solids).

In general, for a spin-unpolarized system, a local-density approximation for the exchange-correlation energy is written as:

$$E_{xc}^{\mathrm{LDA}}[\rho] = \int \rho(\mathbf{r})\epsilon_{xc}(\rho)\ \mathrm{d}\mathbf{r}\ , \tag{2.5}$$

where, ρ is the electronic density and ε_{xc} is the exchange-correlation energy per particle of a homogeneous electron gas of charge density ρ. The exchange-correlation energy is decomposed into exchange and correlation terms linearly,

$$E_{xc} = E_x + E_c\ , \tag{2.6}$$

so that separate expressions for E_x and E_c are sought. The exchange term takes on a simple analytic form for the HEG [15]. Only limiting expressions for the correlation density are known exactly, leading to numerous different approximations for ε_{xc}.

Local-density approximations are important in the construction of more sophisticated approximations to the exchange-correlation energy, such as generalized gradient approximations or hybrid functionals. A desirable property of any approximate exchange-correlation functional is that it reproduce the exact results of the HEG for non-varying densities. As such, LDA's are often an explicit component of such functionals.

2.4 Generalized Gradient Approximations (GGA)

Generalized gradient approximations (GGA) are still local but also take into account the gradient of the density at the same coordinate:

$$E_{XC}^{\mathrm{GGA}}[n_\uparrow, n_\downarrow] = \int \epsilon_{XC}(n_\uparrow, n_\downarrow, \vec{\nabla} n_\uparrow, \vec{\nabla} n_\downarrow) n(\vec{r}) \mathrm{d}^3 r. \tag{2.7}$$

Using the latter (GGA), very good results for molecular geometries and ground-state energies have been achieved [16, 17].

Potentially more accurate than the GGA functionals (Perdew, Burke et al. 1996) are the meta-GGA functionals, a natural development after the GGA (generalized gradient approximation). Meta-GGA DFT functional, in its original form, includes the second derivative of the electron density (the Laplacian) whereas GGA includes only the density and its first derivative in the exchange-correlation potential [18].

Functionals of this type are, for example, TPSS and the Minnesota Functionals. These functionals include a further term in the expansion, depending on the density, the gradient of the density and the Laplacian (second derivative) of the density.

Difficulties in expressing the exchange part of the energy can be relieved by including a component of the exact exchange energy calculated from Hartree–Fock theory. Functionals of this type are known as hybrid functionals.

CHAPTER 3

MATERIALS STUDIO

3.1 Introduction

Materials Studio is a software platform for simulating and modeling materials. It is developed and distributed by Accelrys. This software is used in advanced research of various materials, such as polymers, nanotubes, catalysts, metals, ceramics, and so on, by universities, research centers, and high-technology companies.

Materials Studio is a client–server software package with Microsoft Windows-based PC clients and Windows and Linux-based servers running on PCs, Linux IA-64workstations (including Silicon Graphics (SGI) Altix) and HP XC clusters. There are many modules in Materials Studio. We will now introduce two modules used in this research.

3.2 Materials Studio CASTEP

CASTEP (Cambridge Sequential Total Energy Package) is an *ab initio* quantum mechanical program employing density functional theory (DFT) to simulate the properties of solids, interfaces, and surfaces for a wide range of materials classes such as ceramics, semiconductors, and metals. First principle calculations allow researchers to investigate the nature and origin of the electronic, optical, and structural properties of a system without the need for any experimental input. In that case, Materials Studio CASTEP is the perfect simulation method to research problems in solid state physics, materials science, chemistry, and chemical engineering where empirical models and experimental data are lacking. With the help of CASTEP, researchers can save tremendous of time and costly experiments. CASTEP is capable of computing many electronic, optical, physical properties. In particular, it can predict the electronic properties such as band gaps, density of states and Schottky barriers; optical properties such as reflectivity, absorption, IR spectra, and dielectric functions; or physical properties such as elastic constants and so on.

A total energy plane wave pseudopotential method has been used by Materials Studio CASTEP. In order to reduce the complexity of calculation, core electrons was replaced by effective potentials which acting only on the valence electrons in the system. Electronic wave functions were expanded through a plane-wave basis set, and the local density (LDA) or generalized gradient (GGA) approximations were used to calculate the interaction, exchange and correlation

effects of electrons in the system. Due to the use of pseudopotentials and plane wave basis sets the geometry optimizations of molecules, solids, surfaces, and interfaces are efficient [19].

3.3 Materials Studio DMoL^3

Materials Studio DMoL^3 is one of fastest *ab initio* modeling program that uses density functional theory (DFT) to simulate chemical processes and predict properties of materials. It can predict processes in gas phase, solution, and solid environments, which lead to its great capability to research problems in chemistry, pharmaceuticals, materials science, and chemical engineering, as well as solid state physics.

Using numerical functions on an atom-centered grid as its atomic basis, Materials Studio DMoL^3 achieves its speed and accuracy. By solving the DFT equations for individual atoms the atomic basis functions are obtained. The high quality of these basis sets minimizes basis set superposition effects and allows an improved description of molecular polarizabilities. The electron density in Materials Studio DMoL^3 is expanded in terms of multipolar, atomic-centered partial densities. It provides a compact yet highly accurate representation of the density, and allows for a good scaling with growing system size. Thus, the evaluation of the Coulomb potential and Hamiltonian matrix elements scales linearly with the size of the system. Both all Electron and pseudo-potential calculations can be performed in Materials Studio DMoL^3. Accurate DFT semi-local pseudo-potentials (DSPP) or the more conventional Effective Core Potentials (ECP) can be used. Geometry and transition state optimizations are performed using delocalized internal coordinates, both for molecular as well as for periodic calculations. This includes the ability to impose Cartesian geometry constraints while performing the optimization in internal

coordinates. A transition state search scheme has been applied which is based on a combination of traditional LST/ QST methods. This new robust and fast scheme allows rapid location of transition states. Solvent effects are included using the COSMO model to simulate a continuum [20].

CHAPTER 4

SIMULATION METHOD AND PROCESS

Initially, we created a new project and imported the graphite structure into it.

A graphite structure was constructed by going to File>Import, then selecting Structures>Ceramics>graphite.

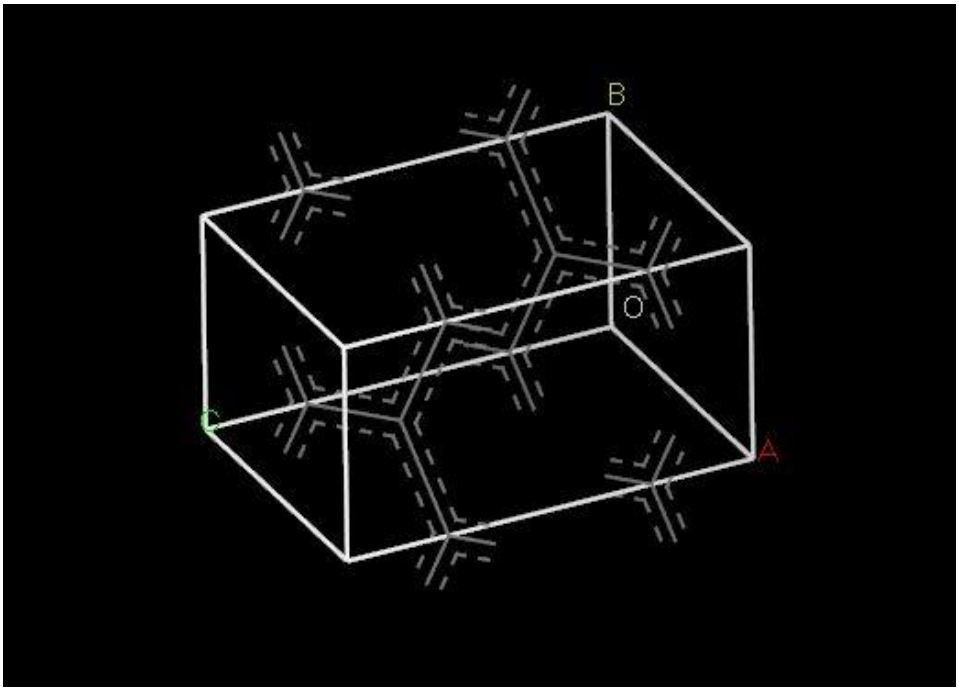

Figure 4.1 Graphite model.

In order to create the graphene sheet structure, some adjustment was needed. First, we utilized Build>Symmetry>Make P1 and then deleted one layer of graphite. This step was to break the symmetry of these two layers so that we could delete one layer without deleting the other layer; so we could build a single layer of graphite or graphene.

Afterwards, we added symmetry back for later calculations. Build>Symmetry>Find symmetry > impose symmetry.

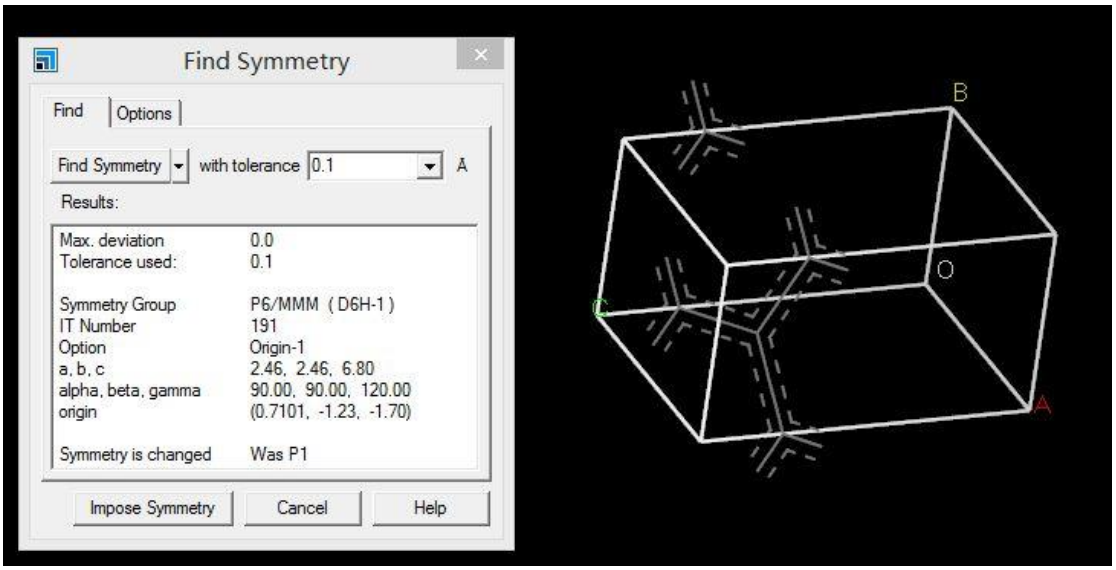

Figure 4.2 Adding symmetry back to the model.

Later, we accessed the honeycomb lattice primitive cell. In order to build the orthogonal graphene sheet, we made the primitive cell 2×2 via Build>Symmetry>supercell. We adjusted its lattice parameters as follows.

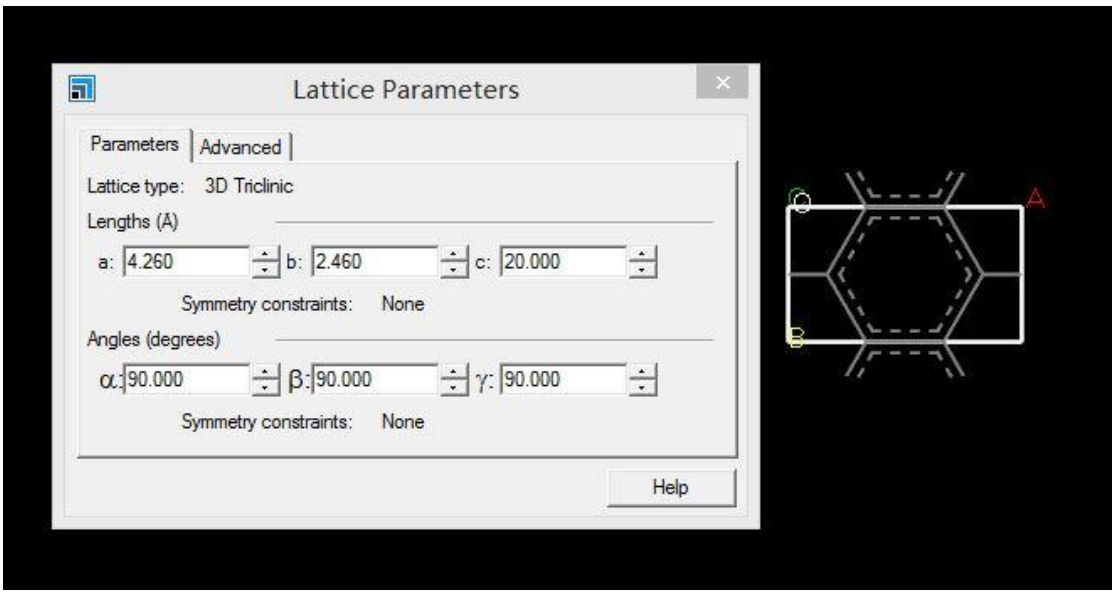

Figure 4.3 Adjustment of lattice parameters.

We made the primitive cell into a graphene sheet using the Supercell option and creating a 4×4 sturcture. Then we selected the whole structure and went to Modify>Modify bond type>partial double bond. Figure 4.4 presents our graphene sheet.

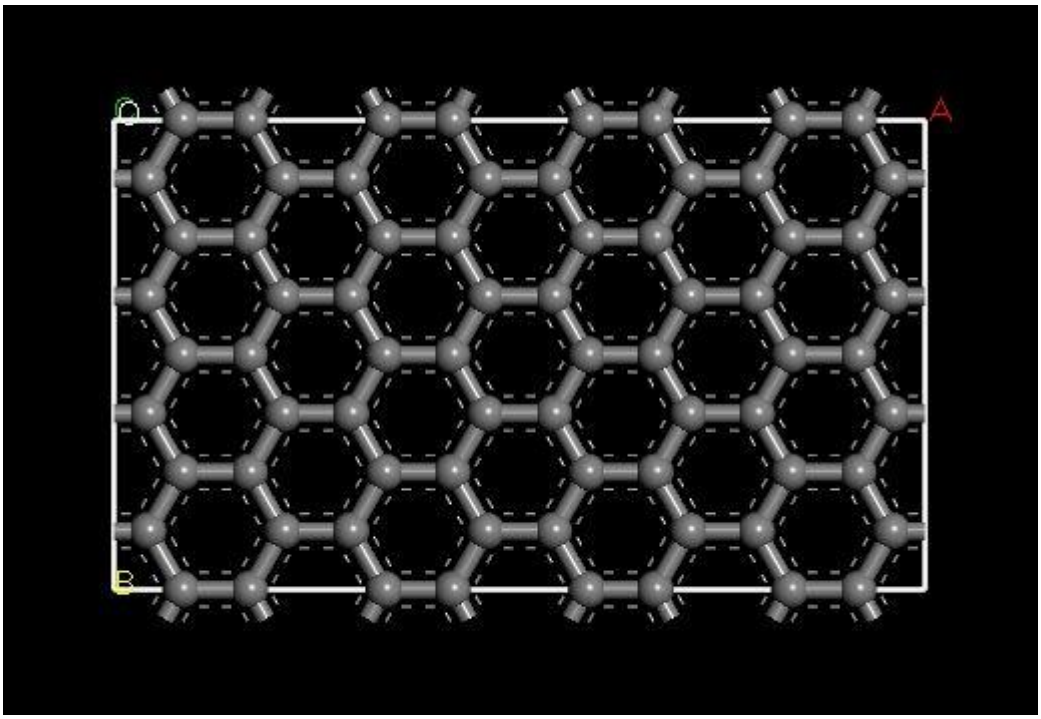

Figure 4.4 Graphene model armchair orientation.

In order to investigate the potential influence on graphene's electronic and optical properties introduced by the defects and number of layers, four models have been created using the same method each time: monolayer graphene, monolayer graphene with defect (containing a single missing carbon atom in the middle for reducing complexity), bilayer graphene and 3-layer-graphene. The calculation setup and results are presented in the next chapter.

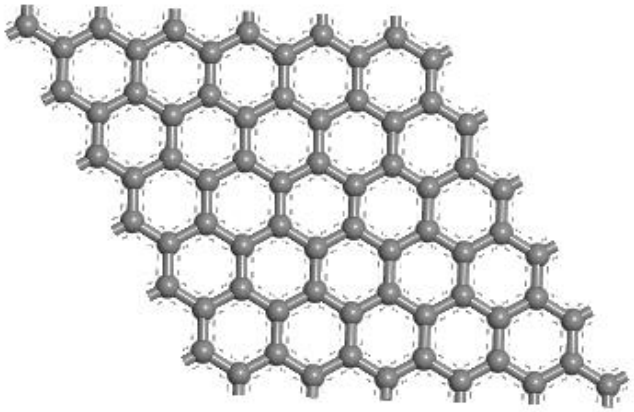

Figure 4.5 Monolayer graphene.

Figure 4.6 Monolayer graphene with defect.

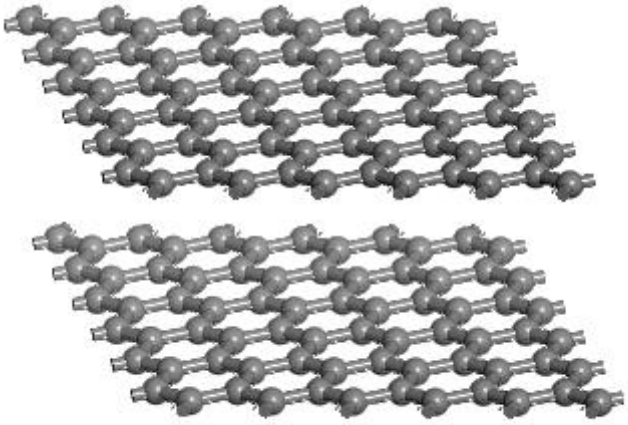

Figure 4.7 Bilayer graphene.

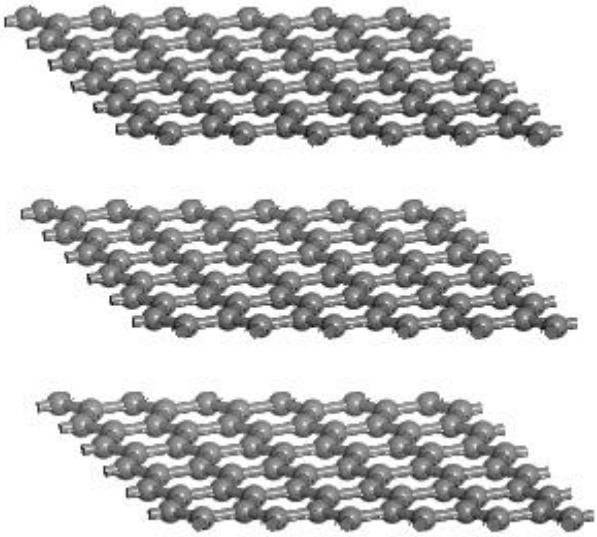

Figure 4.8 3-layer graphene.

CHAPTER 5

RESULTS AND DISCUSSION

The density functional theory (DFT) calculations of energy of these models were performed with Materials Studio CASTEP using norm conserving pseudopotential, plane-wave basis and periodic boundary conditions. The Generalized gradient approximations (GGA) with PW91 functional and a 750 eV cutoff energy for the plane-wave basis set were used in all relaxation processes. The k-point was set to 3 × 3 × 1 for the Brillouin zone integration. The Brillouin zone path was set as G (0.000, 0.000, 0.000) → K (-0.333, 0.667, 0.000) → M (0.000, 0.500, 0.000) → G (0.000, 0.000, 0.000).

The geometry optimization calculations for these models were also carried out via Materials Studio CASTEP modules using norm conserving pseudopotential, plane-wave basis and periodic boundary conditions. The Local density approximations (LDA) with CA-PZ functional and a 750 eV cutoff energy for the plane-wave basis set were used in all relaxation processes. The k-point and Brillouin zone path are the same as above. The reflectivity, absorption and Raman spectrum were calculated in this process.

The calculation results are shown as follows; the band structure of monolayer graphene is approximately linear at or near the Fermi level. The conduction band and valence band intersect with each other at the Fermi level (Figure 5.1) shown as zero band gap which agrees with the theoretical results.

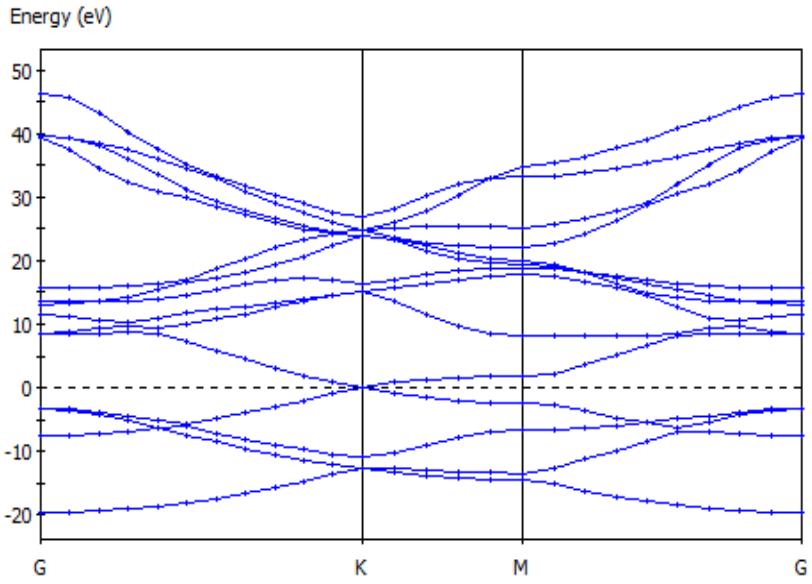

Figure 5.1 Band structure of monolayer graphene.

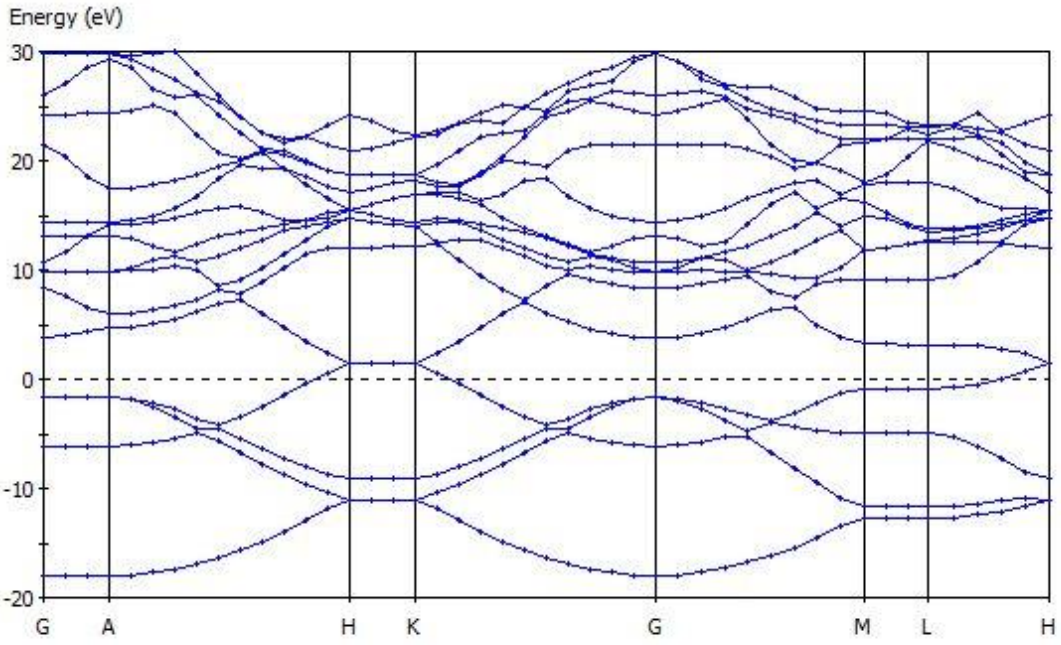

Figure 5.2 Band structure of bilayer and 3-layer graphene.

The band structure of bilayer and 3-layer graphene shows different results from monolayer graphene; it is approximately linear at near Fermi level but the Fermi

level itself has increased by about 1eV. The conduction band and valence band intersect with each other near the Fermi level shown as zero band gap (Figure 5.3). According to our analysis, it should be due to the influence of the other layer of graphene and the orientation.

The density of states describes the number of states per interval of energy at each energy level that are available to be occupied. It is consistent with the band structure. From Figure 5.3, the partial density of states of monolayer graphene, we can see that DOS of monolayer graphene at the Fermi level is very low, about 0, which is consistent with that obtained from the band structure at Fermi level (also 0).

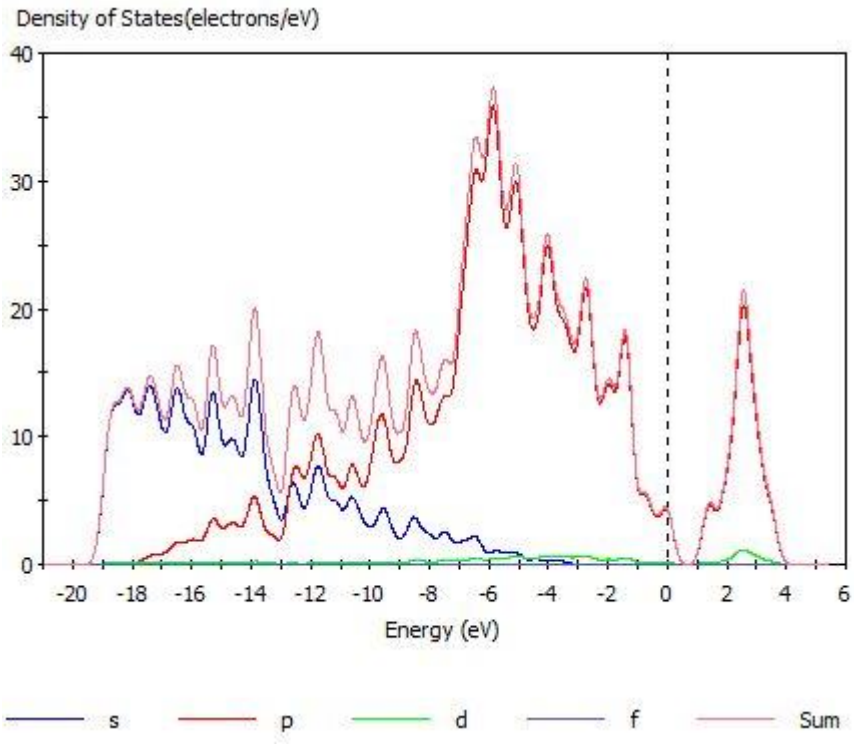

Figure 5.3 The partial density of states of monolayer graphene.

At or near the Fermi level (Figure 5.3), both the DOS and the 2p electrons show some significant peaks, but s electrons almost have no peak at all which means the DOS of graphene is mainly determined by 2p electrons.

For the density of states, as shown in Figures 5.4 and 5.5, bilayer and 3-layer graphene models shows similar results as the sum (of the density of states) in Figure 5.3.

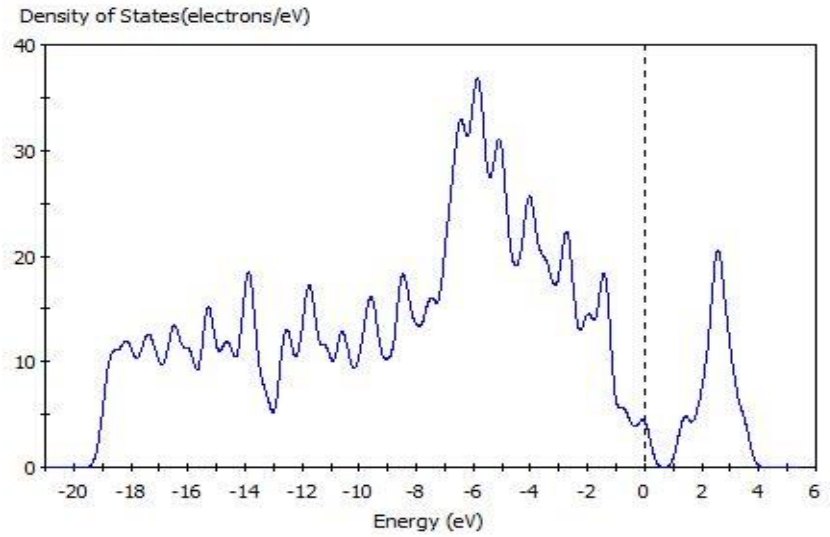

Figure 5.4 Density of states of bilayer graphene.

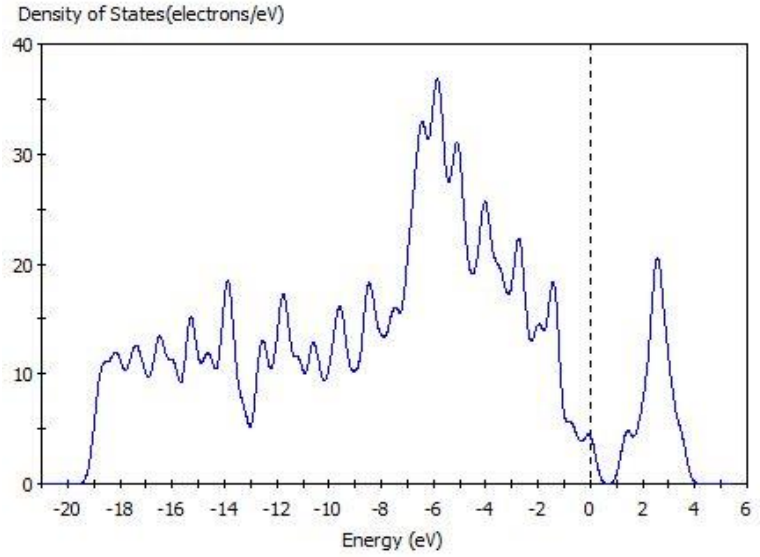

Figure 5.5 Density of state of 3-layer graphene.

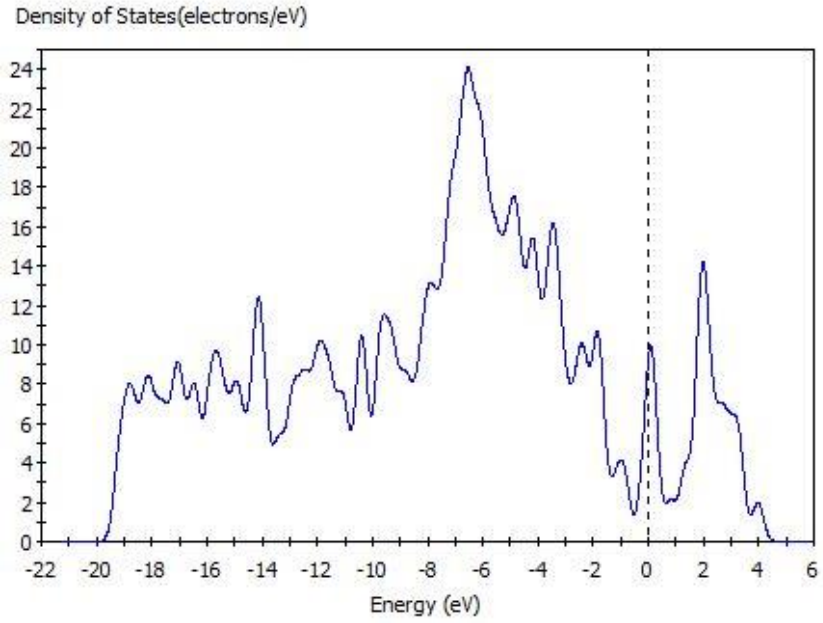

Figure 5.6 DOS of monolayer graphene with defect.

However, the results of the DOS of defect model are different from the above. There is a significant peak at the Fermi level as shown in Figure 5.6. This means the band gap, for the defect model, at the Fermi level is no longer 0, which means the absence of one atom in the graphene sheet has opened a band gap. This phenomenon has also been observed in earlier work [21].

The reflectivity and absorption showed no difference in monolayer, bilayer and 3-layer graphene models, which indicates that at the molecular level, the number of layers has little influence on the optical properties of graphene.

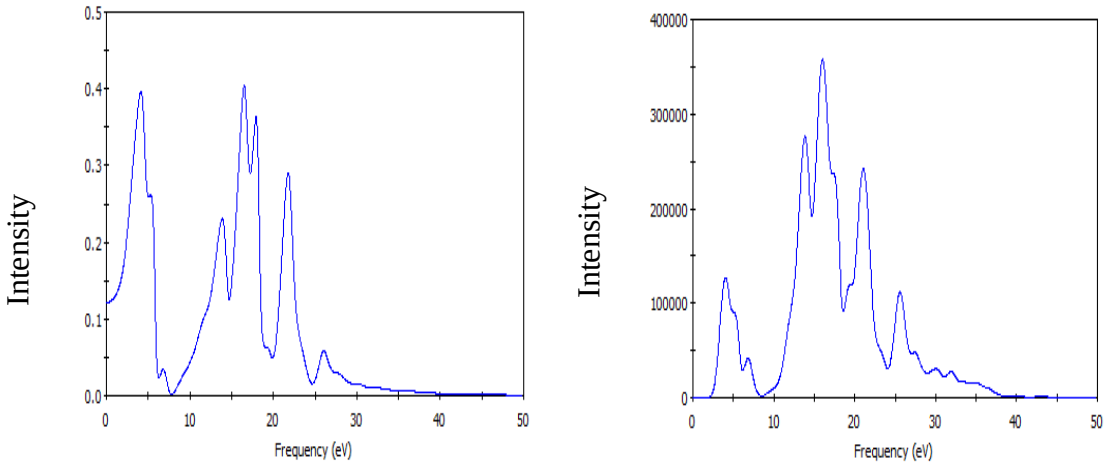

Figure 5.7 Reflectivity and absorption of monolayer graphene (from left to right).

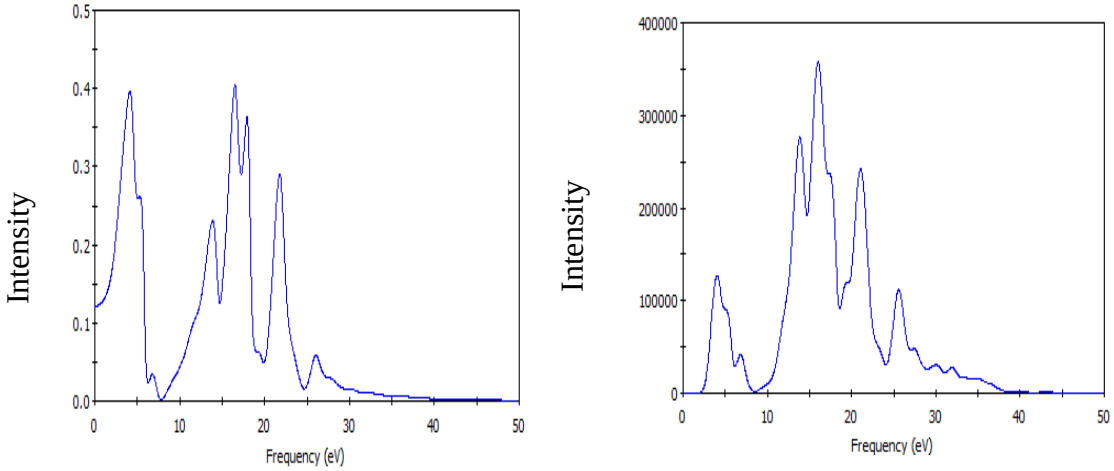

Figure 5.8 Reflectivity and absorption of bilayer graphene (from left to right).

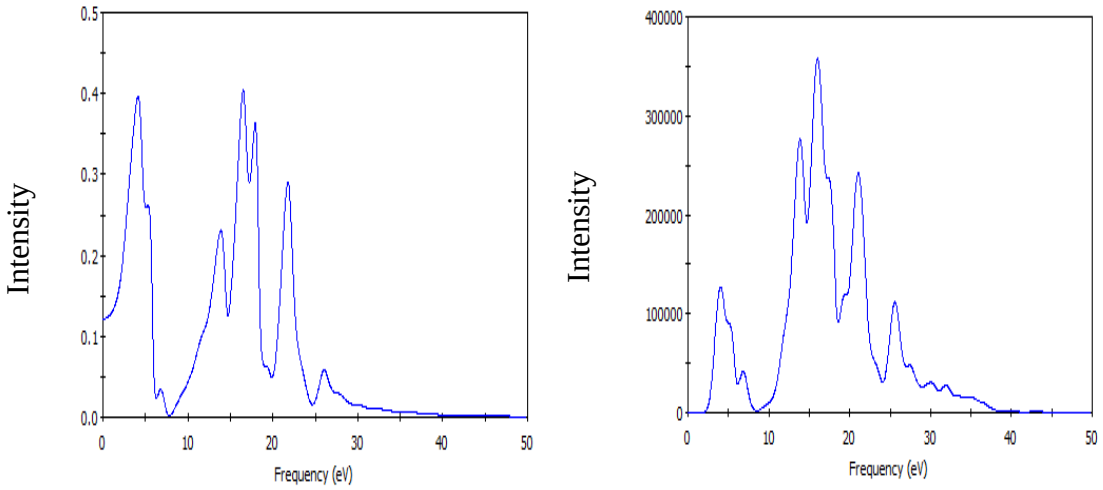

Figure 5.9 Reflectivity and absorption of 3-layer graphene (from left to right).

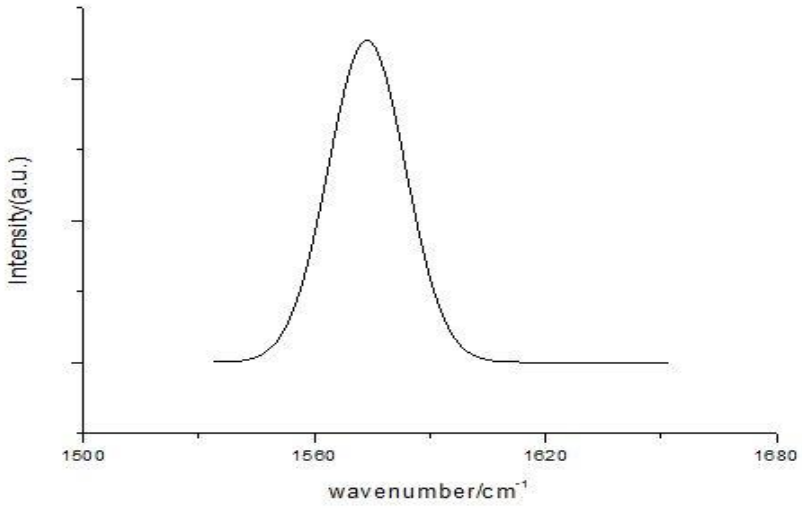

Fig 5.10 Raman spectrum of monolayer graphene.

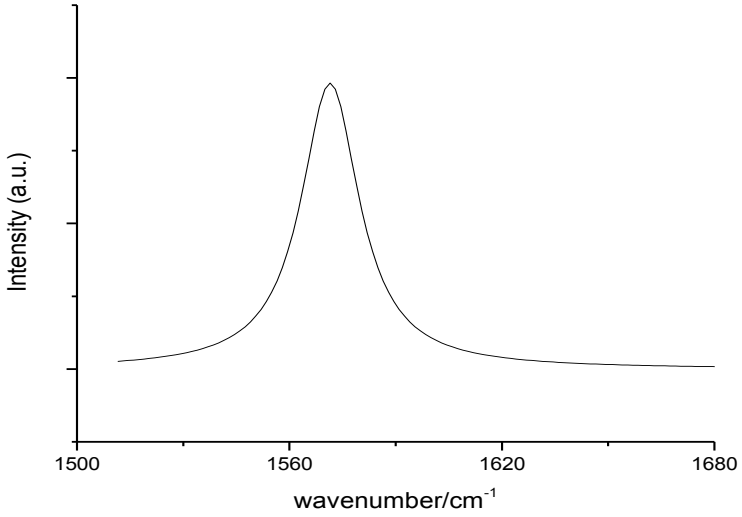

Fig 5.11 Raman spectrum of bilayer graphene.

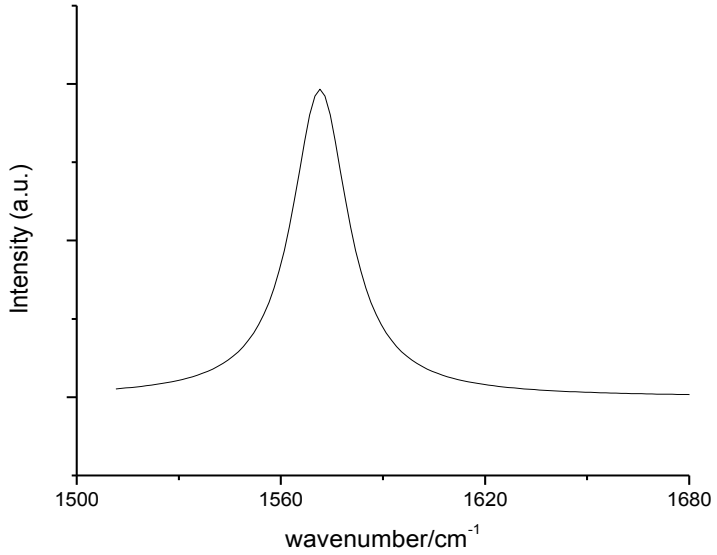

Fig 5.12 Raman spectrum of 3-layer graphene.

The results of the Raman spectrum of the three models is also similar; only one peak can be seen at around 1572.9 cm^{-1} which is consistent with the experimental G peak wavenumber 1583cm^{-1}[22, 23].

CHAPTER 6

CONCLUSIONS

In summary, four different graphene models have been built in this work - monolayer graphene, monolayer graphene with defect, bilayer graphene and 3-layer-graphene. Calculations of the electronic properties and optical properties were performed with Materials Studio CASTEP and Doml[3] modules. With different setting corresponding to energy and geometry optimization calculations, the band structure and density of states have been carried out to study the electronic properties of graphene and investigate of optical properties of different graphene models with a focus on reflectivity, absorption and Raman spectrum.

The band structure of monolayer graphene is approximately linear at or near Fermi level. The conduction band and valence band intersect with each other at the Fermi level and show zero band gap which is in agreement with the theoretical results. For bilayer and 3-layer graphene, the results are similar except the Fermi level has increased due to the influence of the electrons of other layer of graphene.

From density of states (DOS) of monolayer graphene, we can confirm that the major peak was mainly determined by 2p electrons. These peaks, at the DOS of bilayer and 3-layer graphene, show more significance and are distinguishable.

The reflectivity and absorption shown no difference in monolayer, bilayer and 3-layer graphene models. That indicates that, at the molecular level, the number of layers has little influence on the optical properties of graphene.

The Raman spectrum of 3 models has one peak at around 1572.9 cm^{-1} which is about consistent with the experimental G peak wavenumber of 1583cm^{-1}.

Future work will focus on the influence of defects on the optical properties of graphene as well as the effects of electric and magnetic fields on the electronic and optical properties of graphene.

APPENDIX A

MONOLAYER GRAPHENE MODEL INPUT FILE

```
# Task parameters
Calculate                    energy
Symmetry                     on
Max_memory                   2048
File_usage                   smart

# Electronic parameters
Spin_polarization            restricted
Charge                       0
Basis                        dnd
Pseudopotential              none
Functional                   gga(p91)
Aux_density                  octupole
Integration_grid             medium
Occupation                   thermal 0.0050
Cutoff_Global                3.3000 angstrom
Scf_density_convergence      1.0000e-005
Scf_charge_mixing            2.0000e-001
Scf_iterations               50
Scf_diis                     6 pulay

# Kpoint definition file (intervals/offset):
Kpoints                      file        1 1 2 0.0000 0.0000 0.0000
graphene.kpoints

# Calculated properties

Band strucure input file
Calculate                    energy
Scf_iterations               0
use_old_density_and_keep     on
Max_memory                   2048
File_usage                   smart
empty_bands                  12

Symmetry                     on

# Electronic parameters
```

```
Spin_polarization        restricted
Charge                   0
Basis                    dnd
Pseudopotential          none
Functional               gga(p91)
Aux_density              octupole
Integration_grid         medium
Occupation               thermal 0.0050
Cutoff_Global            3.3000 angstrom

# Kpoint definition file:
Kpoints                  file
graphene_BandStr.kpoints

plot_dos                 on

DOS input file
Calculate                energy
Scf_iterations           0
use_old_density_and_keep on
Max_memory               2048
File_usage               smart
empty_bands              12

Symmetry                 on

# Electronic parameters
Spin_polarization        restricted
Charge                   0
Basis                    dnd
Pseudopotential          none
Functional               gga(p91)
Aux_density              octupole
Integration_grid         medium
Occupation               thermal 0.0050
Cutoff_Global            3.3000 angstrom

# Kpoint definition file:
Kpoints                  file        2 2 3 0.000000 0.000000 0.000000
graphene_DOS.kpoints

plot_dos                 on
```

plot_pdos on

Optics input file
comment : CASTEP calculation from Materials Studio
task : GeometryOptimization
xc_functional : PW91
spin_polarized : false
opt_strategy : Default
page_wvfns : 0
cut_off_energy : 750.000000000000000
grid_scale : 1.500000000000000
fine_grid_scale : 1.500000000000000
finite_basis_corr : 2
finite_basis_npoints : 3
elec_energy_tol : 2.000000000000000e-006
max_scf_cycles : 100
fix_occupancy : true
metals_method : dm
mixing_scheme : Pulay
mix_charge_amp : 0.500000000000000
mix_charge_gmax : 1.500000000000000
mix_history_length : 20
nextra_bands : 0
geom_energy_tol : 2.000000000000000e-005
geom_force_tol : 0.050000000000000
geom_stress_tol : 0.100000000000000
geom_disp_tol : 0.002000000000000
geom_max_iter : 100
geom_method : BFGS
fixed_npw : false
geom_modulus_est : 500.000000000000000 GPa
calculate_ELF : false
calculate_stress : true
popn_calculate : true
calculate_hirshfeld : true
calculate_densdiff : false
popn_bond_cutoff : 3.000000000000000
pdos_calculate_weights : false
num_dump_cycles : 0

task : Optics
continuation : default

spin_polarized : false
elec_energy_tol : 2.000000000000000e-006
cut_off_energy : 750.000000000000000
xc_functional : PW91
optics_nextra_bands : 12
bs_eigenvalue_tol : 1.000000000000000e-005
calculate_stress : false
calculate_ELF : false
popn_calculate : false
calculate_hirshfeld : false
calculate_densdiff : false
pdos_calculate_weights : false
num_dump_cycles : 0
bs_write_eigenvalues : true

APPENDIX B

MONOLAYER GRAPHENE WITH DEFECT MODEL INPUT FILE

```
# Task parameters
Calculate                    energy
Symmetry                     on
Max_memory                   2048
File_usage                   smart

# Electronic parameters
Spin_polarization            restricted
Charge                       0
Basis                        dnd
Pseudopotential              none
Functional                   pwc
Harris                       off
Aux_density                  octupole
Integration_grid             medium
Occupation                   thermal 0.0050
Cutoff_Global                3.3000 angstrom
Scf_density_convergence      1.0000e-005
Scf_charge_mixing            2.0000e-001
Scf_iterations               50
Scf_diis                     6 pulay

# Kpoint definition file (intervals/offset):
Kpoints                      file        1 1 2 0.0000 0.0000 0.0000
graphite.kpoints

# Calculated properties

Band structure input file
Calculate                    energy
Scf_iterations               0
use_old_density_and_keep     on
Max_memory                   2048
File_usage                   smart
empty_bands                  12

Symmetry                     on
```

```
# Electronic parameters
Spin_polarization        restricted
Charge                    0
Basis                     dnd
Pseudopotential          none
Functional                pwc
Harris                    off
Aux_density               octupole
Integration_grid         medium
Occupation                thermal 0.0050
Cutoff_Global             3.3000 angstrom

# Kpoint definition file:
Kpoints                   file
graphite_BandStr.kpoints

plot_dos                  on

DOS input file
Calculate                 energy
Scf_iterations           0
use_old_density_and_keep  on
Max_memory                  2048
File_usage                smart
empty_bands               12

Symmetry                   on

# Electronic parameters
Spin_polarization        restricted
Charge                    0
Basis                     dnd
Pseudopotential          none
Functional                pwc
Harris                    off
Aux_density               octupole
Integration_grid         medium
Occupation                thermal 0.0050
Cutoff_Global             3.3000 angstrom

# Kpoint definition file:
Kpoints                   file        2 2 3 0.000000 0.000000 0.000000
```

graphite_DOS.kpoints

plot_dos	on
plot_pdos	on

APPENDIX C

BILAYER GRAPHENE MODEL INPUT FILE

comment : CASTEP calculation from Materials Studio
task : GeometryOptimization
xc_functional : PW91
spin_polarized : false
opt_strategy : Default
page_wvfns : 0
cut_off_energy : 750.000000000000000
grid_scale : 1.500000000000000
fine_grid_scale : 1.500000000000000
finite_basis_corr : 2
finite_basis_npoints : 3
elec_energy_tol : 2.000000000000000e-006
max_scf_cycles : 100
fix_occupancy : true
metals_method : dm
mixing_scheme : Pulay
mix_charge_amp : 0.500000000000000
mix_charge_gmax : 1.500000000000000
mix_history_length : 20
nextra_bands : 0
geom_energy_tol : 2.000000000000000e-005
geom_force_tol : 0.050000000000000
geom_stress_tol : 0.100000000000000
geom_disp_tol : 0.002000000000000
geom_max_iter : 100
geom_method : BFGS
fixed_npw : false
geom_modulus_est : 500.000000000000000 GPa
calculate_ELF : false
calculate_stress : true
popn_calculate : false
calculate_hirshfeld : false
calculate_densdiff : false
pdos_calculate_weights : false
num_dump_cycles : 0

Band structure input file
task : BandStructure
continuation : default

spin_polarized : false
elec_energy_tol : 2.000000000000000e-006
cut_off_energy : 750.000000000000000
xc_functional : PW91
bs_nextra_bands : 12
bs_eigenvalue_tol : 1.000000000000000e-005
calculate_stress : false
calculate_ELF : false
popn_calculate : false
calculate_hirshfeld : false
calculate_densdiff : false
pdos_calculate_weights : false
num_dump_cycles : 0
bs_write_eigenvalues : true

DOS input file
task : BandStructure
continuation : default
spin_polarized : false
elec_energy_tol : 2.000000000000000e-006
cut_off_energy : 750.000000000000000
xc_functional : PW91
bs_nextra_bands : 12
bs_eigenvalue_tol : 1.000000000000000e-005
calculate_stress : false
calculate_ELF : false
popn_calculate : false
calculate_hirshfeld : false
calculate_densdiff : false
pdos_calculate_weights : true
num_dump_cycles : 0
bs_write_eigenvalues : true

Optics input file
task : Optics
continuation : default
spin_polarized : false
elec_energy_tol : 2.000000000000000e-006
cut_off_energy : 750.000000000000000
xc_functional : PW91
optics_nextra_bands : 12
bs_eigenvalue_tol : 1.000000000000000e-005

calculate_stress : false
calculate_ELF : false
popn_calculate : false
calculate_hirshfeld : false
calculate_densdiff : false
pdos_calculate_weights : false
num_dump_cycles : 0
bs_write_eigenvalues : true

APPENDIX D

3-LAYER GRAPHENE MODEL INPUT FILE

comment : CASTEP calculation from Materials Studio
task : GeometryOptimization
xc_functional : LDA
spin_polarized : false
opt_strategy : Default
page_wvfns : 0
cut_off_energy : 750.000000000000000
grid_scale : 1.500000000000000
fine_grid_scale : 1.500000000000000
finite_basis_corr : 2
finite_basis_npoints : 3
elec_energy_tol : 2.000000000000000e-006
max_scf_cycles : 100
fix_occupancy : true
metals_method : dm
mixing_scheme : Pulay
mix_charge_amp : 0.500000000000000
mix_charge_gmax : 1.500000000000000
mix_history_length : 20
nextra_bands : 0
geom_energy_tol : 2.000000000000000e-005
geom_force_tol : 0.050000000000000
geom_stress_tol : 0.100000000000000
geom_disp_tol : 0.002000000000000
geom_max_iter : 100
geom_method : BFGS
fixed_npw : false
geom_modulus_est : 500.000000000000000 GPa
calculate_ELF : false
calculate_stress : true
popn_calculate : true
calculate_hirshfeld : true
calculate_densdiff : false
popn_bond_cutoff : 3.000000000000000
pdos_calculate_weights : false
num_dump_cycles : 0

Band structure input file
task : BandStructure

continuation : default
spin_polarized : false
elec_energy_tol : 2.000000000000000e-006
cut_off_energy : 750.000000000000000
xc_functional : LDA
bs_nextra_bands : 12
bs_eigenvalue_tol : 1.000000000000000e-005
calculate_stress : false
calculate_ELF : false
popn_calculate : false
calculate_hirshfeld : false
calculate_densdiff : false
pdos_calculate_weights : false
num_dump_cycles : 0
bs_write_eigenvalues : true

DOS input file
task : BandStructure
continuation : default
spin_polarized : false
elec_energy_tol : 2.000000000000000e-006
cut_off_energy : 750.000000000000000
xc_functional : LDA
bs_nextra_bands : 12
bs_eigenvalue_tol : 1.000000000000000e-005
calculate_stress : false
calculate_ELF : false
popn_calculate : false
calculate_hirshfeld : false
calculate_densdiff : false
pdos_calculate_weights : true
num_dump_cycles : 0
bs_write_eigenvalues : true

Optics input file
task : Optics
continuation : default
spin_polarized : false
elec_energy_tol : 2.000000000000000e-006
cut_off_energy : 750.000000000000000
xc_functional : LDA
optics_nextra_bands : 12

bs_eigenvalue_tol : 1.000000000000000e-005
calculate_stress : false
calculate_ELF : false
popn_calculate : false
calculate_hirshfeld : false
calculate_densdiff : false
pdos_calculate_weights : false
num_dump_cycles : 0
bs_write_eigenvalues : true

REFERENCES

1. Cooper, D. R., D'Anjou, B., Ghattamaneni, N., Harack, B., Hilke, M., Horth, A., & Yu, V. (2012). Experimental review of graphene. International Scholarly Research Notices, 2012.

2. Factory, A.M.-G. Single Layer Graphene (Graphene Factory). 2015 [cited 2015 April]; Available from: http://www.acsmaterial.com/product.asp?cid=25&id=137.

3. Katsnelson, M. I., & Katsnel′son, M. I. (2012). Graphene: carbon in two dimensions. Cambridge University Press

4. Avouris, P., Chen, Z., & Perebeinos, V. (2007). Carbon-based electronics. Nature nanotechnology, 2(10), 605-615.

5.Novoselov, K. S.; Geim, A. K.; Morozov, S. V.; Jiang, D.; Katsnelson, M. I.; Grigorieva, I. V.; Dubonos, S. V.; Firsov, A. A. (2005). "Two-dimensional gas of massless Dirac fermions in graphene". Nature 438 (7065): 197–200.

6. Kusmartsev, F. V.; Wu, W. M.; Pierpoint, M. P.; Yung, K. C. (2014). "Application of Graphene within Optoelectronic Devices and Transistors".

7. Chen, J. H.; Jang, C.; Adam, S.; Fuhrer, M. S.; Williams, E. D.; Ishigami, M. (2008). "Charged Impurity Scattering in Graphene". Nature Physics 4 (5): 377–381.

8. Fuente, J.d.L. graphene properties. 2014 [cited 2015 April]; Available from: http://www.graphenea.com/pages/graphene-properties#.VUoKxEfF-55.

9. Hohenberg, Pierre; Walter Kohn (1964). "Inhomogeneous electron gas". Physical Review 136 (3B): B864–B871.

10. Vignale, G.; Mark Rasolt (1987). "Density-functional theory in strong magnetic fields". Physical Review Letters (American Physical Society) 59 (20): 2360–2363.

11. Levy, Mel (1979). "Universal variational functionals of electron densities, first-order density matrices, and natural spin-orbitals and solution of the

v-representability problem". Proceedings of the National Academy of Sciences (United States National Academy of Sciences) 76 (12): 6062–6065.

12. Probert, M. (2011). Electronic Structure: Basic Theory and Practical Methods, by Richard M. Martin: Scope: graduate level textbook. Level: theoretical materials scientists/condensed matter physicists/computational chemists.

13. Kohn, Walter; Sham, Lu Jeu (1965). "Self-Consistent Equations Including Exchange and Correlation Effects".

14. Parr, Robert G.; Yang, Weitao (1994). Density-Functional Theory of Atoms and Molecules.

15. Perdew, John P; Chevary, J A; Vosko, S H; Jackson, Koblar, A; Pederson, Mark R; Singh, D J; Fiolhais, Carlos (1992). "Atoms, molecules, solids, and surfaces: Applications of the generalized gradient approximation for exchange and correlation". Physical Review B46 (11): 6671.

16. Perdew, J. P., et al. (1996). "Generalized Gradient Approximation Made Simple." Physical Review Letters 77(18): 3865-3868.

17. Becke, Axel D (1988). "Density-functional exchange-energy approximation with correct asymptotic behavior". Physical Review A 38 (6): 3098.

18. Langreth, David C; Mehl, M J (1983). "Beyond the local-density approximation in calculations of ground-state electronic properties". Physical Review B 28 (4): 1809.

19. Accelrys. CASTEP-DATASHEET. 2014 [cited 2015 April]; Available from: http://accelrys.com/products/datasheets/castep.pdf.

20. Accelrys. BIOVIA MATERIALS STUDIO DMOL3. 2014 [cited 2015 April]; Available from: http://accelrys.com/products/datasheets/dmol3.pdf.

21. Zhang, Y. H., Chen, Y. B., Zhou, K. G., Liu, C. H., Zeng, J., Zhang, H. L., & Peng, Y. (2009). "Improving gas sensing properties of graphene by introducing dopants and defects: a first-principles study". Nanotechnology, 20(18), 185504.

22. Bo, L., Hongjuan, S., & Pengtong, J. (2012). "Factor Group Analysis of Molecular Vibrational Modes of Graphene and Density Functional Calculations". Acta Phys.- Chim. Sin, 28.

23. Ferrari, A. C., Meyer, J. C., Scardaci, V., Casiraghi, C., Lazzeri, M., Mauri, F., Piscanec, S., Jiang, D., Novoselov, K.S., Roth, S, & Geim, A. K. (2006). "Raman spectrum of graphene and graphene layers". Physical review letters, 97(18), 187401.